Application of a Probabilistic Neural Network in radial velocity curve analysis of the spectroscopic binary stars Schulte 3, HD 37366, HD 195987, HD 101131 and HD 93205

K. Ghaderi[1*] **and A. Pirkhedri**[2]

[1] *Islamic Azad University, Marivan Branch, Department of Science, Marivan, Iran*

[2] *Islamic Azad University, Marivan Branch, Department of Computer Engineering, Marivan, Iran*

Using measured radial velocity data of five double-lined spectroscopic binary systems Schulte 3, HD 37366, HD 195987, HD 101131 and HD 93205, we find corresponding orbital and spectroscopic elements via a Probabilistic Neural Network (PNN). Our numerical results are in good agreement with those obtained by others using more traditional methods.

PACS numbers: 97.80.Hn, 97.80.Fk

Key words: Stars: binaries: eclipsing – Stars: binaries: spectroscopic

1. Introduction

Analysis of both light and radial velocity (hereafter V_R) curves of binary systems helps us to determine the masses and radii of individual stars. One historically well-known method to analyze the V_R curve is that of Lehmann-Filhés [1]. Some other methods were also introduced by Sterne [2] and Petrie [3]. The different methods of the V_R curve analysis have been reviewed in ample detail by Karami & Teimoorinia [4]. Karami & Teimoorinia [4] also proposed a new non-linear least squares velocity curve analysis technique for spectroscopic binary stars. They showed the validity of their new method to a wide range of different types of binary See Karami & Mohebi [5-7] and Karami et al. [8].

Probabilistic Neural Network (PNN) is a new tool to derive the orbital parameters of the spectroscopic binary stars. In this method the time consumed is considerably less than the method of Lehmann-Filhés and even less than the non-linear regression method proposed by Karami & Teimoorinia [4].

In the present paper we use a Probabilistic Neural Network (PNN) to find the optimum match to the four parameters of the V_R curves of the five double-lined spectroscopic binary systems: Schulte 3, HD 37366, HD 195987, HD 101131 and

* Electronic address: K.Ghaderi.60 @ gmail.com

HD 93205. Our aim is to show the validity of our new method to a wide range of different types of binary.

Schulte 3 is a double-lined eclipsing binary and it is a probable member of Cyg OB2. The spectral type is O6IV and O9III for the primary and the secondary star, respectively, and the orbital period is P =4.7464 days [9]. HD 37366 is a double-lined spectroscopic binary with a period of P =31.8188 days. The primary of HD 37366 is classified as O9.5 V, and it contributes approximately two-thirds of the optical flux. The less luminous secondary is a broad-lined, early B-type main-sequence star [10]. HD 195987 is a moderately metal-poor double-lined binary system with an orbital period of P =57.32161 days. The continuum from the secondary typically tends to fill in the spectral lines of the primary, which then appear weaker as if the star were more metal-poor and the combined-light photometry is reddened [11]. HD 101131 is a brightest objects in the young open cluster IC 2944. This system is a double-lined spectroscopic binary in an elliptical orbit with a period of P= 9.64659 days. It is a young system (approximately 2 million years old) and The spectral type is O6.5 V((f)) and O8.5 V for the primary and the secondary star , respectively [12]. HD 93205 is an O-type spectroscopic binary and The spectral type is O3V and O8V for the primary and the secondary star, respectively, and the orbital period is P=6.0803 days [13].

This paper is organized as follows. In Sect. 2, we introduce a Probabilistic Neural Network (PNN) to estimate the four parameters of the V_R curve. In Sect. 3, the numerical results are reported, while the conclusions are given in Sect. 4.

2. V_R curve parameters estimation by the Probabilistic Neural Network (PNN)

Following Smart [14], the V_R of a star in a binary system is defined as follows

$$\mathrm{V_R} = \gamma + K[\cos(\theta + \omega) + e\cos\omega], \tag{1}$$

where γ is the V_R of the center of mass of system with respect to the sun. Also K is the amplitude of the V_R of the star with respect to the center of mass of the binary. Furthermore θ, ω and e are the angular polar coordinate (true anomaly), the longitude of periastron and the eccentricity, respectively.

Here we apply the PNN method to estimate the four orbital parameters, γ, K, e and ω of the V_R curve in Eq. (1). In this work, for the identification of the observational V_R curves, the input vector is the fitted V_R curve of a star. The PNN is first trained to classify V_R curves corresponding to all the possible combinations of γ, K, e and ω. For this one can synthetically generate V_R curves given by Eq. (1) for each combination of the parameters:

- $-100 \leq \gamma \leq 100$ in steps of 1;
- $1 \leq K \leq 300$ in steps of 1;

– $0 \leq e \leq 1$ in steps of 0.001;

– $0 \leq \omega \leq 360^\circ$ in steps of 5.

This gives a very big set of k pattern groups, where k denotes the number of different V_R classes, one class for each combination of γ, K, e and ω. Since this very big number of different V_R classes causes to some computational limitations, hence one can first start with the big step sizes. Note that from Petrie [3], one can guess γ, K and e from a V_R curve. This enable one to limit the range of parameters around their initial guesses. When the preliminary orbit was derived after several stages, then one can use the above small step sizes to obtain the final orbit. The PNN has four layer including input, pattern, summation, and output layers, respectively (see Fig. 5 in Bazarghan et al. [15]). When an input vector is presented, the pattern layer computes distances from the input vector to the training input vectors and produces a vector whose elements indicate how close the input is to a training input. The summation layer sums these contributions for each class of inputs to produce as its net output a vector of probabilities. Finally, a competitive transfer function on the output layer picks the maximum of these probabilities, and produces a 1 for that class and a 0 for the other classes [16,17]. Thus, the PNN classifies the input vector into a specific k class labeled by the four parameters γ, K, e and ω because that class has the maximum probability of being correct.

3. Numerical Results

Here, we use the PNN to derive the orbital elements for the five different double-lined spectroscopic systems Schulte 3, HD 37366, HD 195987, HD 101131 and HD 93205. Using measured V_R data of the two components of these systems obtained by Kiminki et al. [9] for Schulte 3, Boyajian et al. [10] for HD 37366, Torres et al. [11] for HD 195987, Gies et al. [12] for HD 101131 and Morrell et al. [13] for HD 93205, the fitted velocity curves are plotted in terms of the photometric phase in Figs. 1 to 5.

The orbital parameters obtaining from the PNN for Schulte 3, HD 37366, HD 195987, HD 101131 and HD 93205 are tabulated in Tables 1, 3, 5, 7 and 9, respectively. Tables show that the results are in good accordance with the those obtained by Kiminki et al. [9] for Schulte 3, Boyajian et al. [10] for HD 37366, Torres et al. [11] for HD 195987, Gies et al. [12] for HD 101131 and Morrell et al. [13] for HD 93205.

Note that the Gaussian errors of the orbital parameters in Tables 1, 3, 5, 7 and 9 are the same selected steps for generating V_R curves, i.e. $\Delta\gamma = 1, \Delta K = 1, \Delta e = 0.001$ and $\Delta\omega = 5$. These are close to the observational errors reported in the literature. Regarding the estimated errors, following Specht [17], the error of the decision boundaries depends on the accuracy with which the underlying Probability Density Functions (PDFs) are estimated. Parzen [18] proved that

the expected error gets smaller as the estimate is based on a large data set. This definition of consistency is particularly important since it means that the true distribution will be approached in a smooth manner. Specht [17] showed that a very large value of the smoothing parameter would cause the estimated errors to be Gaussian regardless of the true underlying distribution and the misclassification rate is stable and does not change dramatically with small changes in the smoothing parameter.

The combined spectroscopic elements including $m_p \sin^3 i$, $m_s \sin^3 i$, $(m_p + m_s) \sin^3 i$, $(a_p + a_s) \sin i$ and m_s/m_p are calculated by substituting the estimated parameters K, e and ω into Eqs. (3), (15) and (16) in Karami and Teimoorinia [4]. The results obtained for the five systems are tabulated in Tables 2, 4, 6, 8 and 10 show that our results are in good agreement with the those obtained by Kiminki et al. [9] for Schulte 3, Boyajian et al. [10] for HD 37366, Torres et al. [11] for HD 195987, Gies et al. [12] for HD 101131 and Morrell et al. [13] for HD 93205, respectively. Here the errors of the combined spectroscopic elements in Tables 2, 4, 6, 8 and 10 are obtained by the help of orbital parameters errors. See again Eqs. (3), (15) and (16) in Karami and Teimoorinia [4].

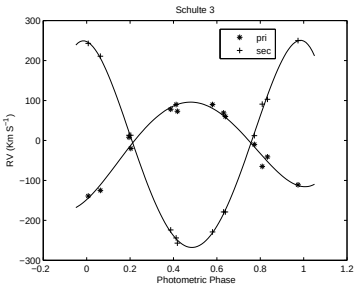

Figure 1. Radial velocities of the primary and secondary components of Schulte 3 plotted against the photometric phase. The observational data have been measured by Kiminki et al. [9].

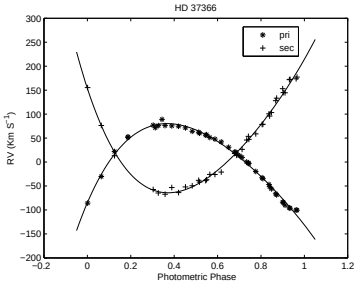

Figure 2. Radial velocities of the primary and secondary components of HD 37366 plotted against the photometric phase. The observational data have been measured by Boyajian et al. [10].

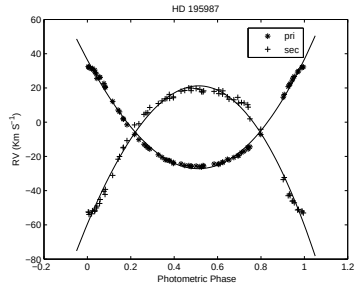

Figure 3. Radial velocities of the primary and secondary components of HD 195987 plotted against the photometric phase. The observational data have been measured by Torres et al. [11].

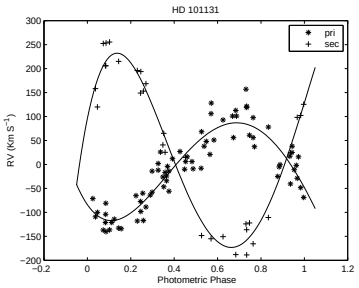

Figure 4. Radial velocities of the primary and secondary components of HD 101131 plotted against the photometric phase. The observational data have been measured by Gies et al. [12].

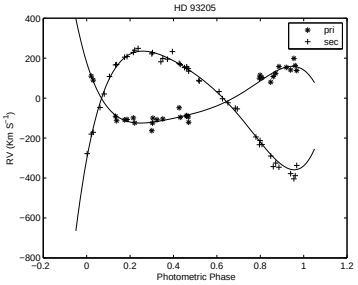

Figure 5. Radial velocities of the primary and secondary components of HD 93205 plotted against the photometric phase. The observational data have been measured by Morrell et al. [13].

Table 1. Orbital parameters of Schulte 3

	This Paper	Kiminki et al. [9]
$\gamma\left(kms^{-1}\right)$	-26 ± 1	$-26.4(1.7)$
$K_p\left(kms^{-1}\right)$	113 ± 1	$113.2(14.5)$
$K_s\left(kms^{-1}\right)$	257 ± 1	$256.7(2.4)$
e	0.071 ± 0.001	$0.070(0.009)$
$\omega(^\circ)$	10 ± 5	$5.5(0.7)$

Table 2. Combined spectroscopic elements of Schulte 3

Parameter	This Paper	Kiminki et al. [9]
$m_p \sin^3 i/M_\odot$	17.1707 ± 0.0019	—
$m_s \sin^3 i/M_\odot$	7.5498 ± 0.0015	—
$(m_p + m_s) \sin^3 i/M_\odot$	24.7205 ± 0.0034	—
$a_p \sin i/R_\odot$	7.8855 ± 0.0692	7.4(0.9)
$a_s \sin i/R_\odot$	17.9343 ± 0.0685	16.7(0.2)
$(a_p + a_s) \sin i/R_\odot$	25.8197 ± 0.1377	—
m_s/m_p	0.4397 ± 0.0113	—

Table 3. Orbital parameters of HD 37366

	This Paper	Boyajian et al. [10]
$\gamma_p \left(kms^{-1}\right)$	18 ± 1	13.3 ± 0.2
$\gamma_s \left(kms^{-1}\right)$	18 ± 1	21.6 ± 0.9
$K_p \left(kms^{-1}\right)$	89 ± 1	88.7 ± 0.2
$K_s \left(kms^{-1}\right)$	118 ± 1	117.4 ± 1.2
e	0.331 ± 0.001	$0.330(fixed)$
$\omega(^\circ)$	210 ± 5	$211.6(fixed)$

Table 4. Combined spectroscopic elements of HD 37366

Parameter	This Paper	Boyajian et al. [10]
$m_p \sin^3 i/M_\odot$	14.0053 ± 0.0007	13.9 ± 0.3
$m_s \sin^3 i/M_\odot$	10.5633 ± 0.0006	10.42 ± 0.08
$(m_p + m_s) \sin^3 i/M_\odot$	24.5687 ± 0.0014	—
$a_p \sin i/R_\odot$	52.7734 ± 0.5733	52.62 ± 0.13
$a_s \sin i/R_\odot$	69.9692 ± 0.5669	69.7 ± 0.7
$(a_p + a_s) \sin i/R_\odot$	122.7426 ± 1.1403	—
m_s/m_p	0.7542 ± 0.0037	—

Table 5. Orbital parameters of HD 195987

	This Paper	Torres et al. [11]
$\gamma\left(kms^{-1}\right)$	-5 ± 1	-5.867 ± 0.038
$K_p\left(kms^{-1}\right)$	29 ± 1	28.944 ± 0.046
$K_s\left(kms^{-1}\right)$	37 ± 1	36.73 ± 0.21
e	0.310 ± 0.001	0.3103 ± 0.0018
$\omega(^\circ)$	355 ± 5	357.03 ± 0.35

Table 6. Combined spectroscopic elements of HD 195987

Parameter	This Paper	Torres et al. [11]
$m_p \sin^3 i/M_\odot$	0.8226 ± 0.002	0.808 ± 0.010
$m_s \sin^3 i/M_\odot$	0.6447 ± 0.0002	0.6369 ± 0.0046
$(m_p + m_s) \sin^3 i/M_\odot$	1.4673 ± 0.0004	—
$a_p \sin i/10^6 km$	21.7437 ± 0.7423	21.689 ± 0.036
$a_s \sin i/10^6 km$	27.7420 ± 0.7403	27.52 ± 0.16
$(a_p + a_s) \sin i/R_\odot$	71.0332 ± 2.1282	70.70 ± 0.24
m_s/m_p	0.7838 ± 0.0095	0.7881 ± 0.0047

Table 7. Orbital parameters of HD 101131

	This Paper	Gies et al. [12]
$\gamma_p\left(kms^{-1}\right)$	6 ± 1	-4.9 (25)
$\gamma_s\left(kms^{-1}\right)$	6 ± 1	11 (5)
$K_p\left(kms^{-1}\right)$	118 ± 1	117 (4)
$K_s\left(kms^{-1}\right)$	210 ± 1	211 (7)
e	0.155 ± 0.001	0.156 (29)
$\omega(^\circ)$	125 ± 5	122 (12)

Table 8. Combined spectroscopic elements of HD 101131

Parameter	This Paper	Gies et al. [12]
$m_p \sin^3 i/M_\odot$	21.7710 ± 0.0014	21.8 (21)
$m_s \sin^3 i/M_\odot$	12.2332 ± 0.0012	12.1 (13)
$(m_p + m_s) \sin^3 i/M_\odot$	34.0043 ± 0.0026	—
$a_p \sin i/R_\odot$	22.2082 ± 0.1847	22.0 (7)
$a_s \sin i/R_\odot$	39.5231 ± 0.1819	39.7 (12)
$(a_p + a_s) \sin i/R_\odot$	61.7314 ± 0.3666	—
m_s/m_p	0.5619 ± 0.0066	—

Table 9. Orbital parameters of HD 93205

	This Paper	Morrell et al. [13]
$\gamma \left(kms^{-1}\right)$	-9 ± 1	-8.8 ± 1.3
$K_p \left(kms^{-1}\right)$	145 ± 1	144.5 ± 2.6
$K_s \left(kms^{-1}\right)$	312 ± 1	312.1 ± 2.5
e	0.371 ± 0.001	0.37 ± 0.01
$\omega(^\circ)$	55 ± 5	52.0 ± 1.3

Table 10. Combined spectroscopic elements of HD 93205

Parameter	This Paper	Morrell et al. [13]
$m_p \sin^3 i/M_\odot$	32.8719 ± 0.0018	33.0 ± 1.6
$m_s \sin^3 i/M_\odot$	15.2770 ± 0.0014	15.3 ± 1.5
$(m_p + m_s) \sin^3 i/M_\odot$	48.1489 ± 0.0033	—
$a_p \sin i/10^6 km$	11.2640 ± 0.0728	11.2 ± 0.2
$a_s \sin i/10^6 km$	24.2371 ± 0.0673	24.3 ± 0.3
$(a_p + a_s) \sin i/10^6 km$	35.5011 ± 0.1401	—
m_s/m_p	0.4647 ± 0.0079	0.463 ± 0.012

4. Conclusions

a Probabilistic Neural Network to derive the orbital elements of spectroscopic binary stars was applied. PNNs are used in both regression (including parameter estimation) and classification problems. However, one can discretize a continuous regression problem to such a degree that it can be represented as a classification problem [16,17], as we did in this work.

Using the measured V_R data of Schulte 3, HD 37366, HD 195987, HD 101131 and HD 93205 obtained by Kiminki et al. [9], Boyajian et al. [10], Torres et al. [11], Gies et al. [12] and Morrell et al. [13], respectively, we find the orbital elements of these systems by the PNN. Our numerical results shows that the results obtained for the orbital and spectroscopic parameters are in good agreement with those obtained by others using more traditional methods.

This method is applicable to orbits of all eccentricities and inclination angles. In this method the time consumed is considerably less than the method of Lehmann-Filhés. It is also more accurate as the orbital elements are deduced from all points of the velocity curve instead of four in the method of Lehmann-Filhés. The present method enables one to vary all of the unknown parameters γ , K, e and ω simultaneously instead of one or two of them at a time. It is possible to make adjustments in the elements before the final result is obtained. There are some cases, for which the geometrical methods are inapplicable, and in these cases the present one may be found useful. One such case would occur when observations are incomplete because certain phases could not have been observed. Another case in which this method is useful is that of a star attended by two dark companions with commensurable periods. In this case the resultant velocity curve may have several unequal maxima and the geometrical methods fail altogether.

Acknowledgements. This work has been supported financially by Islamic Azad University, Marivan Branch, Iran.

References

[1] R. Lehmann-Filhés, AN. **136**, 17 (1984).
[2] T. E. Sterne, PNAS. **27**, 175 (1941).
[3] R. M. Petrie, "Astronomical Techniques," Ed., W. A. Hiltner, University of Chicago Press, Chicago (1960).
[4] K. Karami and H. Teimoorinia, Ap&SS. **311**, 435 (2007).
[5] K. Karami and R. Mohebi, ChJAA. **7**, 668 (2007).
[6] K. Karami and R. Mohebi, JApA. **28**, 217 (2007).
[7] K. Karami and R. Mohebi, JApA. **30**, 153 (2009).
[8] K. Karami, R. Mohebi and M. M. Soltanzadeh, Ap&SS. **318**, 69 (2008).
[9] D. C. Kiminki, M. V. McSwain and H. A. Kobulnicky, ApJ. **679**, 1478 (2008).

[10] T. S. Boyajian, D. R. Gies, J. P. Dunn, C. D. Farrington, E. D. Grundstrom, W. Huang, M. V. McSwain, S. J. Williams, D. W. Wingert, A. W. Fullerton and C. T. Bolton, ApJ. **664**, 1121 (2007).
[11] G. Torres, A. F. Boden, D. W. Latham, M. Pan and R. P. Stefanik, AJ. **124**, 1716 (2002).
[12] D. R. Gies, L. R. Penny, P. Mayer, H. Drechsel and R. Lorenz, ApJ. **574**, 957 (2002).
[13] N. I. Morrell, R. H. Barba, V. S. Niemela, M. A. Corti, J. F. Albacete Colombo, G. Rauw, M. Corcoran, T. Morel, J. F. Bertrand, A. F .J. Moffat and N. St-Louis, MNRAS. **326**, 85 (2001).
[14] W. M. Smart, "Textbook on Spherical Astronomy," Sixth Ed., Revised by R. M. Green , Cambridge Univ. Press, 360 (1990).
[15] M. Bazarghan, H. Safari, D. E. Innes, E. Karami and S. K. Solanki, A&A, **492**, L13 (2008).
[16] D. F. Specht, "in Proc IEEE International Conference on Neural Networks," 525 (1988).
[17] D. F. Specht, Neural Networks, **3**, 109 (1990).
[18] E. Parzen, Annals of Mathematical Statistics, **33**, 1065 (1962).